

Improving LADCP Velocity with External Heading, Pitch, and Roll

A. M. THURNHERR

Lamont-Doherty Earth Observatory, Columbia University, Palisades, New York

I. GOSZCZKO

Institute of Oceanology, Polish Academy of Sciences, Sopot, Poland

F. BAHR

Woods Hole Oceanographic Institution, Woods Hole, Massachusetts

(Manuscript received 30 December 2016, in final form 18 April 2017)

ABSTRACT


Data collected with acoustic Doppler current profilers installed on CTD rosettes and lowered through the water column [lowered ADCP (LADCP) systems] are routinely used to derive full-depth profiles of ocean velocity. In addition to the uncertainties arising from random noise in the along-beam velocity measurements, LADCP-derived velocities are commonly contaminated by bias errors due to imperfectly measured instrument attitude (heading, pitch, and roll). Of particular concern are the heading measurements, because it is not usually feasible to calibrate the internal ADCP compasses with the instruments installed on a CTD rosette, away from the magnetic disturbances of the ship. Heading data from dual-headed LADCP systems, which consist of upward- and downward-pointing ADCPs installed on the same rosette, commonly indicate heading-dependent compass errors with amplitudes exceeding 10° . In an attempt to reduce LADCP velocity errors, several dozen profiles of simultaneous LADCP and magnetometer/accelerometer data were collected in the Gulf of Mexico. Agreement between the LADCP profiles and simultaneous shipboard velocity measurements improves significantly when the former are processed with external attitude measurements. Another set of LADCP profiles with external attitude data was collected in a region of the Arctic Ocean where the horizontal geomagnetic field is too weak for the ADCP compasses to work reliably. Good agreement between shipboard velocity measurements and Arctic LADCP profiles collected at magnetic dip angles exceeding 87° and processed with external attitude measurements indicate that high-quality velocity profiles can be obtained close to the magnetic poles.

1. Introduction

Acoustic Doppler velocity profilers (ADCPs) mounted on CTD rosettes—so-called lowered ADCP (LADCP) systems—are routinely used to collect velocity profiles in the ocean. LADCP data have been processed for horizontal velocity for over two decades (Fischer and Visbeck 1993). More recently, a method has been developed to obtain vertical ocean velocity as well (Thurnherr 2011). LADCP-derived velocities can

be used directly, for example, for circulation studies (e.g., Thurnherr et al. 2011; St. Laurent et al. 2012). Importantly, LADCP velocities can also be used to estimate turbulence and mixing levels using so-called finestructure parameterization methods (Gregg 1989; Polzin et al. 2014; Thurnherr et al. 2015).

Lowered ADCP work puts high demands on the instruments. For horizontal velocity, the ADCP measurements must be sufficiently accurate so that the errors in vertical shear, integrated over the full profile depths, do not exceed a few centimeters per second (cm s^{-1} ; Firing and Gordon 1990). For vertical velocity, the ADCP measurements must be sufficiently accurate to yield signals of a few millimeters per second (mm s^{-1}) from a platform moving up to $\approx 2 \text{ m s}^{-1}$ (Thurnherr 2011). Given these demands, it is important that any measurement errors show as little bias as possible. One area of particular

 Denotes content that is immediately available upon publication as open access.

Corresponding author: Andreas M. Thurnherr, ant@ldeo.columbia.edu

concern with regard to ADCP velocity bias is the measurements of instrument attitude (heading, pitch and roll). These data are required to transform the velocity measurements from a coordinate system aligned with the instrument into the conventional u , v , and w components (Earth coordinates). From LADCP data collected with “dual headed” systems (two ADCPs on a rosette, one pointing upward and the other downward; Visbeck 2002), it is clear that compass measurements in particular are associated with large uncertainties that sometimes exceed 15° . The underlying problem is that it is not generally feasible to carry out ADCP compass calibrations on fully loaded rosettes, away from the magnetic disturbances of the ship. Therefore, LADCP work is usually carried out with nominal compass calibrations. Another problem with many LADCP profiles is that the measurements are often made at large package tilts (deviations from the vertical), especially in regions of strong currents or during tow-yo casts. At large package angles, tilt measurement errors become more important. For some commonly used instruments, compass errors increase with increasing instrument tilts, further emphasizing the need for high-quality pitch and roll measurements.

Here, we analyze two LADCP datasets that were collected with additional external accelerometer/magnetometer measurements (section 2). Large instrument tilts due to very strong upper-ocean currents adversely affect many of the profiles in the first set, collected in the northeastern Gulf of Mexico (section 3). When processed with the external attitude measurements, the differences between the corresponding LADCP and shipboard ADCP (SADCP) velocities decrease by $\approx 20\%$. In the second set of profiles (section 4), most of the ADCP data do not contain any valid heading information because they were collected in a region of the Arctic Ocean where the earth’s geomagnetic field lines are inclined too steeply for the ADCP compasses to work reliably. Based on a comparison with shipboard ADCP velocities, at least 85% of the corresponding profiles processed with the external attitude data are of high quality. The main implications of the new technique are discussed in section 5.

2. Methods

a. Magnetometer and accelerometer measurements

A simple instrument called the Independent Measurement Package (IMP; Fig. 1) was built using a datalogger connected to inexpensive magnetometer/accelerometer chips that are readily available as robotics components [so-called inertial measurement unit (IMU) breakout boards]. In its present configuration, the IMP collects

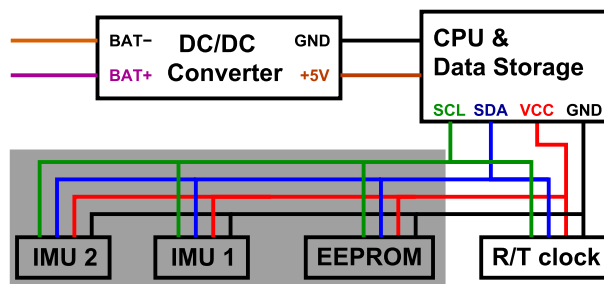


FIG. 1. Schematic of the IMP. CPU and data storage are provided by a Raspberry Pi microcontroller running the Arch Linux operating system and public domain firmware that is available on request. Several peripherals are attached to the CPU via a simple two-wire interintegrated circuit (I^2C) bus: 1) A real-time clock (Macetech ChronoDot), 2) Robotics breakout boards based on the LSM303DLHC and LSM303D accelerometer/magnetometer chips (labeled IMU1 and IMU2, respectively), and 3) A 128-byte EEPROM; microchip 24AA02E48) for sensor configuration and usage logging. In the most recent incarnation of the IMP, the components on the gray background are housed in a separate small pressure case that can be mounted away from any magnetic disturbances.

magnetometer/accelerometer data from two microchips manufactured by STMicroelectronics: the LSM303DLHC and the similar, but somewhat more recent, LSM303D. The IMP records 100-Hz time series of all three components of acceleration and the magnetic field strength in a coordinate system that is aligned with the sensor chips. In a first step, the data are despiked with a five-wide ($1/20$ s) median filter and bin averaged to 5 Hz, primarily to reduce file size. Next, the data are low passed with a simple frequency-domain filter with a 2-s cutoff, because high-frequency motion is highly damped underwater.

From the filtered time series of acceleration A_x , A_y , and A_z , estimates for pitch ϕ and roll ρ are calculated using

$$\tan\phi = \frac{-A_x}{\sqrt{A_y^2 + A_z^2}}, \quad \text{and} \quad (1)$$

$$\tan\rho = \frac{A_y}{A_z}, \quad (2)$$

respectively. Note that, similar to the ADCP pitch/roll measurements, ϕ and ρ are equal to the true pitch and roll angles, respectively, only in the absence of horizontal acceleration. Because of large lateral drag of submerged CTD rosettes, horizontal acceleration can be neglected.¹ Both accelerometer and magnetometer

¹This assertion was tested with an Xsens IMU that distinguishes between instrument tilt and horizontal acceleration, and that was deployed on a CTD rosette during two casts in rough seas in the Southern Ocean during the 2010 DIMES second U.K. (UK2) cruise (rms horizontal acceleration $< 0.5 \text{ m}^2 \text{ s}^{-1}$).

data are corrected for pitch and roll, that is, rotated into a vertical coordinate system. In case of the accelerometer data, this yields a time series of vertical acceleration, as horizontal acceleration is null by construction. Rotating the magnetometer data yields the two horizontal components of the measured magnetic field M_x and M_y , which are used for compass calibration. The total measured field strength $M_t = \sqrt{M_x^2 + M_y^2 + M_z^2}$ is also useful for detecting erroneous measurements, including those near the surface affected by the ship's magnetic field.

b. Compass calibration

In the absence of external disturbances, the magnetic field vector at a given location on the earth's surface is approximately constant on the short time scales typical of LADCP casts, with horizontal field strength $M_h \equiv \sqrt{M_x^2 + M_y^2}$, although there is diurnal polar wander that can affect compass measurements very close to the magnetic poles on time scales of hours (Hamilton 2001). When this constant field is measured with a horizontally rotating magnetometer, the resulting measurements of M_y , when plotted against the corresponding M_x , lie on a circle with radius M_h centered at the origin. There are two types of magnetic (including electromagnetic) disturbances that can contaminate geomagnetic field measurements: so-called hard-iron and soft-iron effects. Hard-iron effects can be thought of as resulting from a permanent magnet corotating with the magnetometer. The resulting magnetic field causes fixed (i.e., heading independent) biases in M_x and M_y —the measurements still fall on a circle with radius M_h , but this circle is now offset from the origin. In contrast to hard-iron effects, soft-iron effects vary with magnetometer orientation (heading)—their effect is to distort the measurement circle into an ellipse. Algorithmically, compass calibration consists of mapping the measured M_x/M_y ellipse into a circle centered at the origin. In practice, hard-iron effects typically dominate, in which case compass calibration amounts to determining biases for the two horizontal magnetometer components, which is easily done from visual inspection of plots. From the calibrated horizontal magnetometer data, heading η is calculated using

$$\tan \eta = \frac{M_y}{M_x}. \quad (3)$$

The compass calibration procedure described here assumes that the magnetic disturbances remain constant during a profile. Significant deviations from the “calibration circle” indicate either magnetometer measurement

errors or time-varying magnetic disturbances and are used for LADCP data editing.

c. Merging ADCP data with external attitude measurements

To calculate the replacement values for the ADCP attitude data from external measurements, the relative alignment of the external sensors with respect to the ADCP transducer must be known. Here, the offset angles are calculated from in situ profile data with the following simple algorithm:

- 1) For both instruments (ADCP and IMP), subtract the mean instrument tilts from the measured data, that is, replace pitch and roll with their temporal anomalies.
- 2) Using the pitch/roll time series from both instruments, calculate the corresponding time series of the instrument tilt angle (from vertical) and azimuth (heading).
- 3) Use temporal lag correlation to determine the clock difference between the corresponding time series of tilt magnitude, which are independent of the heading offset between the instruments.
- 4) Determine the heading offset between the IMP and the ADCP pitch/roll sensors from the differences between the two corresponding tilt–azimuth estimates.
- 5) Use this heading offset to rotate the external pitch/roll measurements into the coordinate frame of the ADCP. (The differences between the rotated mean tilts give the pitch/roll offsets of the external accelerometers with respect to the ADCP, but these are not required.)
- 6) Construct replacement time series for ADCP pitch and roll by adding the rotated external pitch/roll anomalies to the corresponding ADCP means determined in step 1; construct a replacement time series for ADCP heading by adding the heading offset determined in step 4 to the external heading time series.

If necessary, data from multiple profiles can be combined to determine the instrument alignment (steps 1–4), as long as the instruments have not been moved on the rosette between the profiles.

To avoid having to modify multiple LADCP processing software packages to work with the external attitude data, “patched” binary ADCP data files are created by replacing the pitch, roll, and heading data with the corresponding replacement time series from the IMP. Ensembles without valid external heading measurements are effectively removed from the data files by marking the corresponding velocity measurements as

invalid. For LADCP data collected in Earth coordinates, before processing the velocities also have to be transformed back to beam coordinates, which is accomplished by inverting the rotation matrices of the beam-to-instrument and instrument-to-Earth transformations (RD Instruments 1998).

d. LADCP data processing and quality control

The LADCP data are processed for horizontal velocity with the LDEO_IX implementation of the velocity inversion method (Visbeck 2002). The profiles are processed without the SADCP referencing constraint, that is, using only the ship drift (GPS) and bottom tracking (where available) to constrain the barotropic velocities. With this processing, rms differences between the LADCP profiles and simultaneous on-station SADCP velocities from the upper ocean can be used to quantify the uncertainty of the LADCP measurements (Thurnherr 2010). High-quality LADCP datasets typically have LADCP–SADCP velocity differences between 2 and $\approx 6 \text{ cm s}^{-1}$. The dataset collected with a dual-headed LADCP system (section 3) was also processed for vertical velocity using the method of Thurnherr (2011); differences between the resulting single-instrument profiles were used for a secondary quality assessment.

3. ECOGIG EN586 data

In July 2016, 42 LADCP/CTD/IMP profiles were collected in the northeastern Gulf of Mexico during the R/V *Endeavor* EN586 cruise of the Gulf of Mexico Research Initiative (GoMRI)-funded Ecosystem Impacts of Oil and Gas Inputs to the Gulf (ECOGIG-2) program. Two Teledyne RD Instruments (TRDI) 300-kHz Workhorse ADCPs, recording beam-coordinate velocities in 6-m bins without blanking, were installed on the CTD rosette together with an IMP. A TRDI 75-kHz Ocean Surveyer SADCP measured the velocity field in the upper $\approx 800 \text{ m}$. The sampling region was strongly affected by a large loop eddy with horizontal velocities in the upper ocean sometimes exceeding 1 m s^{-1} . As a result many of the profiles, including the one shown in Fig. 2, were collected at large instrument tilts. All ECOGIG profiles show evidence of large heading-dependent differences between the compasses of the two ADCPs. In the example shown in the top-left panel in Fig. 2, the CTD package performed a full rotation during the cast, providing compass differences for all headings. Peak compass differences exceed 10° in the heading ranges 80° – 150° , and 230° – 300° , that is, over $\approx 40\%$ of the entire heading range.

Compass calibration was carried out by subtracting visually determined M_x and M_y magnetometer biases

from the horizontal field measurements; Fig. 3 shows an example. The approximate circularity of the data implies that soft-iron effects are small and can be ignored. Since the IMP pressure case was removed from the CTD rosette for battery changes twice during the cruise, three separate magnetometer calibrations were carried out. After bias calibration, the velocities of all ADCP ensembles with horizontal field strengths that deviate by more than 20% from the nominal calibration circle are marked bad. The bad samples (green dots in Fig. 3) are primarily from the deployment and recovery and include on-deck time. Influence of the surface-ship's magnetic field is detected down to 50 m in this dataset. A comparison of the corresponding magnetometer-calibration plots from the two sensor chips indicates that the horizontal field magnitude is measured more consistently with the older LSM303DLHC chip (there is less scatter in the red samples in the left panel of Fig. 3). On the other hand, instrument alignment is constrained significantly more tightly with the data from the newer LSM303D chip (see below), which is therefore used for all the results shown below.

A positive consequence of the large tilt angles in the EN586 profiles is that the relative instrument alignment is very tightly constrained by pitch and roll data. The profiles from each of the three magnetometer calibrations (between battery changes) were combined to determine the mean heading offsets between the instruments for each installation of the IMP. For the LSM303D chip, the corresponding standard errors lie between 0.4° and 1.2° ; for the LSM303DLHC chip, the errors range between 0.6° and 2.1° . The mean relative heading offset between the two ADCPs, inferred from the three profile groups, is $98.2^\circ \pm 0.5^\circ$ for the LSM303D chip and $99.0^\circ \pm 2.4^\circ$ for the LSM303DLHC chip. With the former, the accuracy of the heading offsets is constrained to within 0.5° ; with the latter, the uncertainty is about 5 times larger.

Using the instrument alignment offsets to construct replacement heading time series for the ADCPs yields estimates for the heading-dependent compass errors of the two instruments (Fig. 4). These estimates indicate that the heading differences shown in Fig. 2 are dominated by errors in the uplooker compass.

Significantly improved consistency between the data from the two ADCPs is readily apparent when processing the EN586 profiles with external attitude measurements. In particular, there are no longer any heading-dependent compass offsets, and the pitch and roll differences show reduced scatter (Fig. 2). In many profiles, there is less spatial structure in the inversion residuals from horizontal-velocity processing (Visbeck 2002) when external attitude data are used,

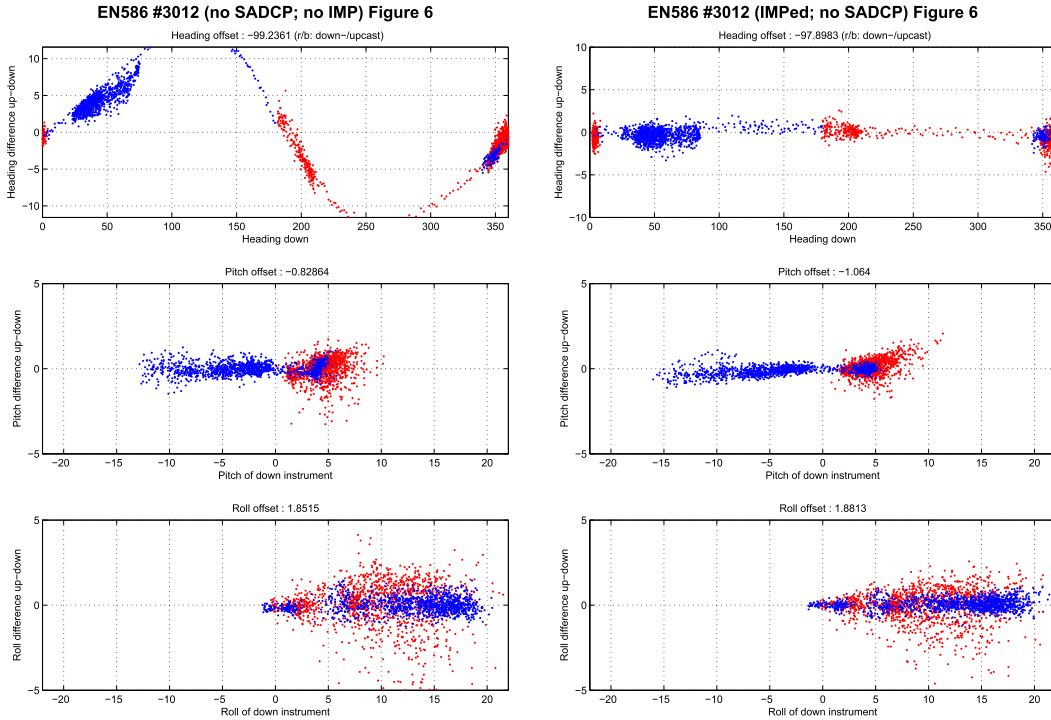


FIG. 2. Differences between uplooker and downlooker measurements of (top) heading, (middle) pitch, and (bottom) roll from an example profile from the ECOGIG EN586 cruise showing downcast data (red samples) and upcast data (blue samples). (left) Processed with ADCP attitude data. (right) Processed with IMP attitude data.

indicating that the measurement errors are more random (not shown).

More importantly, the LADCP velocities processed with external attitude data agree more closely with the corresponding SADCP velocities than the original

profiles (Fig. 5). Averaged over the entire dataset, external attitude measurements improve the rms differences between the LADCP and SADCP velocities by $\approx 10\%$; an improvement of $\approx 20\%$ is achieved when outliers with velocity differences $> 0.12 \text{ m s}^{-1}$ are excluded.

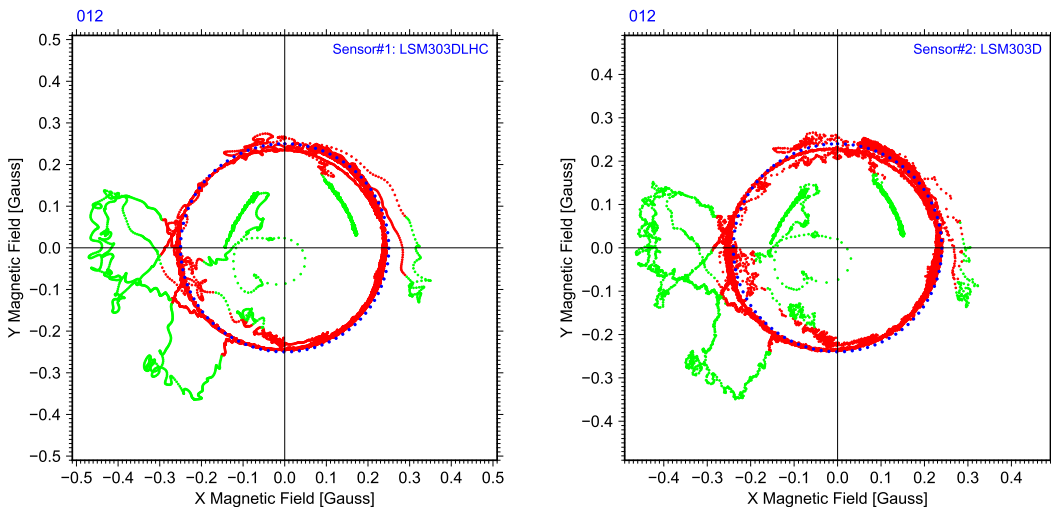


FIG. 3. Postcalibration horizontal magnetic field data from a yo-yo cast (three profiles) that includes the profile shown in Fig. 2. Shown are the calibration circle (blue dots) and horizontal field strengths within 20% of the calibration circle (red samples); green samples have field strengths with greater deviations. (left) From (older) the LSM303DLHC chip, and (right) from the LSM303D chip.

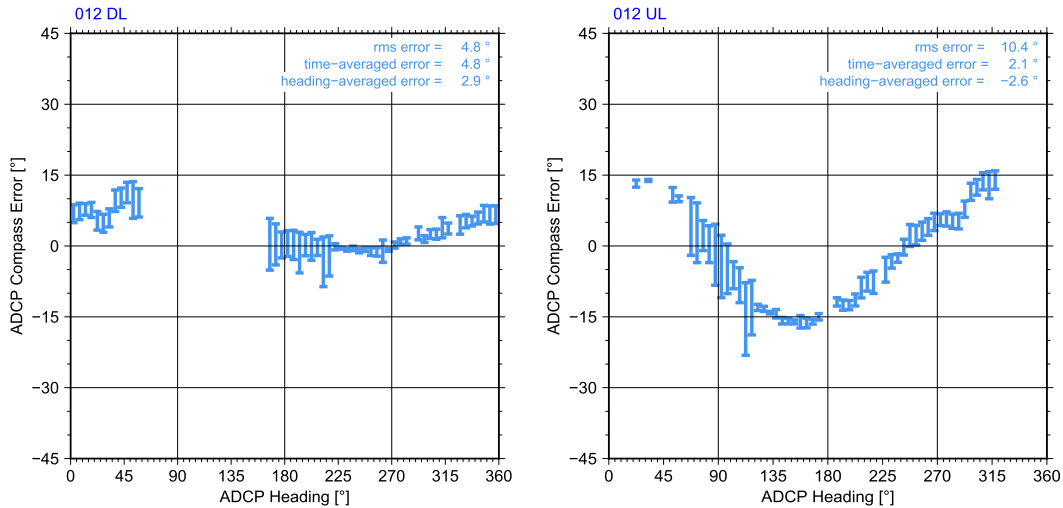


FIG. 4. Heading-averaged ADCP compass errors and standard deviations in the yo-yo profile shown in Fig. 3; headings collected at instrument tilts $>10^\circ$ are not used. (left) Downlooker ADCP and (right) uplooker ADCP.

The LADCP-derived *vertical* velocities in the ECOGIG dataset also improve when processed with external attitude measurements, noting that only pitch and roll matter in this case because vertical velocity does not require any heading data (Thurnherr 2011). In case of the ECOGIG profiles, the vertical-velocity differences between the two instruments decreases by $\approx 10\%$ in the upcasts, whereas there are no apparent improvements in the downcasts (not shown). This difference is likely due to greater pitching motion during upcasts, because the package is dragged against the horizontal currents (rather than drifting with the currents during downcasts) and because of bottle-stop winch accelerations.

4. NABOS 2015 data

In September 2015, 70 LADCP/CTD/IMP profiles were collected in the Arctic Ocean along the Russian margin of the Nansen and Amundsen basins (75° – 83° N, 64° – 178° E) during the second cruise of the international Nansen and Amundsen Basins Observational System (NABOS-II) monitoring program. A single TRDI 300-kHz Workhorse, recording Earth coordinate velocities in 10-m bins with 2-m blanking, was installed in a downward-facing orientation on the CTD rosette together with an IMP. A TRDI 75-kHz Ocean Surveyer SADCP measured the velocity field in the upper 500–600 m. The sampling region is characterized by a weak horizontal geomagnetic field $H_f \approx 0.02$ – 0.06 G, which is significantly below the 0.1G (=10000 nT) manufacturer limit for TRDI Workhorse compasses. Consequently, there are large differences between the corresponding ADCP- and IMP-derived heading time series in nearly

all of the profiles (Fig. 6). Most have heading-dependent ADCP compass errors with peak values exceeding 30° , as illustrated by the example in the left panel. In some extreme cases, the ADCP compass indicates a narrow range of headings (i.e., “weathervaning”), even though the IMP data show that the instrument performed at least one full rotation (right panel). This behavior occurs when the magnitude of the horizontal magnetometer biases exceeds the horizontal geomagnetic field strength, in which case the measurements of M_y plotted against M_x no longer encompass the origin. Out of the

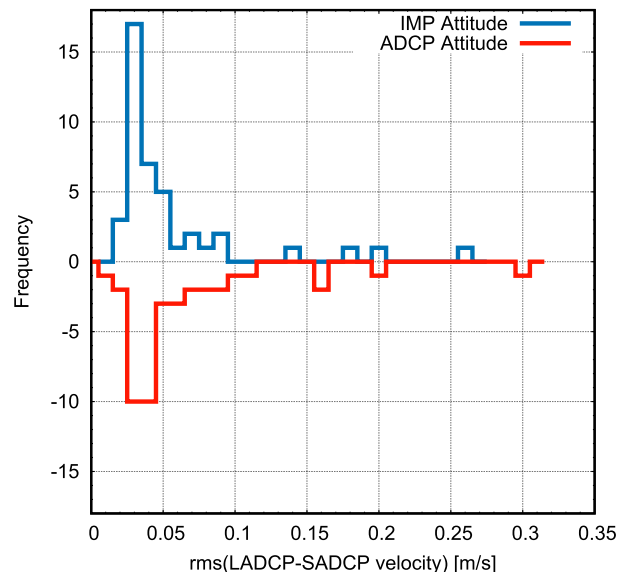


FIG. 5. Histograms of the profile-averaged rms differences between the corresponding upper-ocean LADCP and SADCP velocities in the ECOGIG data.

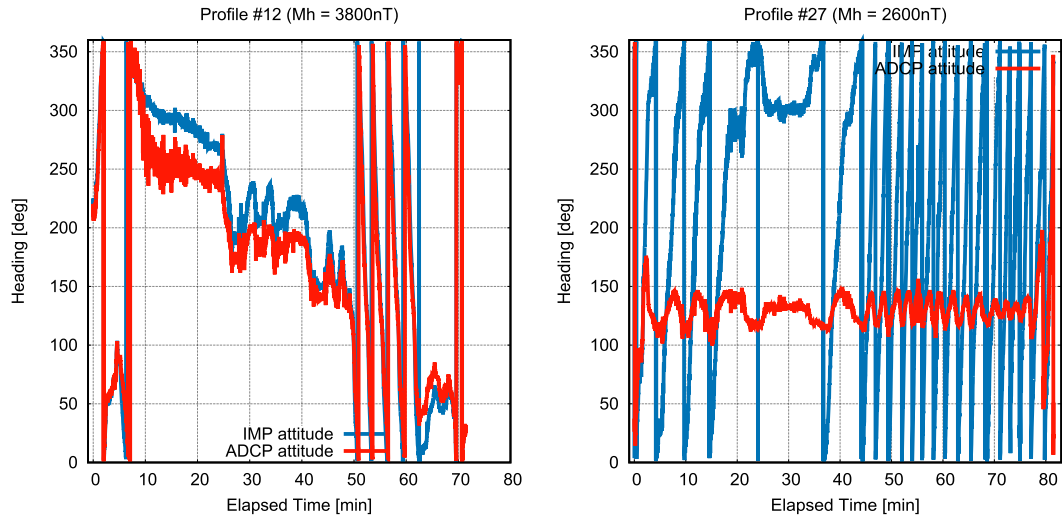


FIG. 6. Heading time series from NABOS profiles (left) 12 and (right) 27. ADCP-derived headings (red) and IMP-derived headings (blue). Horizontal geomagnetic field strength is printed above each panel; the corresponding field inclinations are 86.4° and 87.6° , respectively.

70 NABOS profiles, 9 (i.e., fewer than 15%) have acceptable ADCP-derived heading time series (compass errors similar to those shown in Fig. 4). Interestingly, almost half (four) out of those nine were collected at stations with horizontal field magnitudes below that of profile 27 (right panel). From this we infer that geomagnetic field strength is not the only factor affecting the performance of TRDI Workhorse compasses; the available data suggest that performance degrades with increasing sea state (see below).

For the NABOS profiles, magnetometer calibration was again carried out by visually determining M_x and M_y biases; Fig. 7 shows two examples. Soft-iron effects are

ignored as before. Because the horizontal geomagnetic field strength varies by factor of 3 across the sampling region, 42 separate magnetometer calibrations were carried out. As before, magnetic field measurements that deviate more than a set percentage (25% in this case) from the nominal calibration circles are marked invalid (green samples in the figure). The elevated magnetometer scatter apparent in profile 27 is a consequence of the heightened sea state (large pitch and roll). The green samples inside the calibration circle in this profile were recorded between 50 and 100 m below the sea surface during the upcast. As magnetic effects of the ship can be detected down to 100 m in many of the

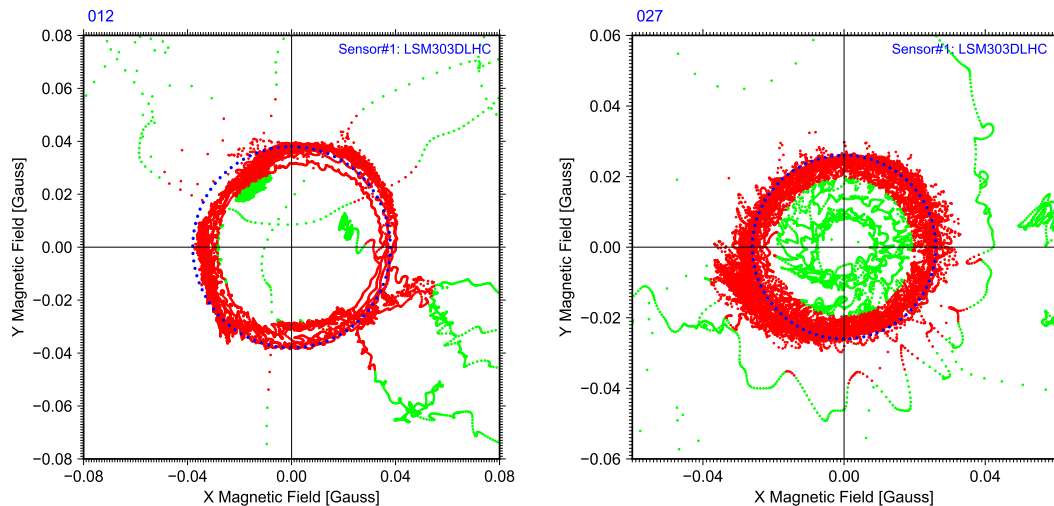


FIG. 7. Magnetometer calibration for NABOS profiles (left) 12 and (right) 27. Shown are the calibration circle (blue dots) and horizontal field strengths within 20% of the calibration circle (red samples); green samples have field strengths with greater deviations.

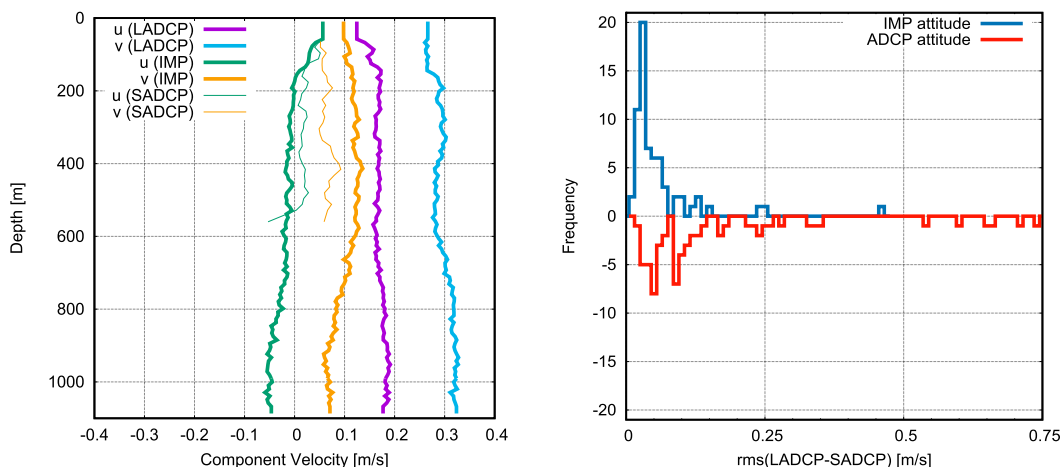


FIG. 8. LADCP vs SADCPC velocities in the NABOS data. (left) Velocities of profile 27. Because of magnetic contamination from the ship, there are no valid velocity samples in the top 60 m of the water column; the processing software extrapolates the uppermost valid velocity sample to the surface. (right) Histograms of the rms LADCP vs SADCPC velocity differences from all profiles.

profiles from this dataset (not shown), we attribute the low- H_f anomalies to this effect as well. Similar to the ECOGIG measurements, the data from the older LSM303DLHC sensor show considerably less scatter than those from the newer LSM303D chip (not shown).

During collection of the NABOS profiles, neither of the instruments was moved onto the CTD rosette. Excluding two shallow profiles, the mean heading offset between the ADCP transducer and the IMP accelerometer is $99.7^\circ \pm 0.2^\circ$; that is, for this dataset, too, instrument alignment is determined from in situ data to an accuracy better than 1° .

Many of the original NABOS LADCP profiles, when processed without external attitude data, show differences exceeding 0.1 m s^{-1} compared to the corresponding SADCPC velocities (Fig. 8). In these profiles there are typically no apparent similarities between the SADCPC and the corresponding LADCP velocities in the upper ocean (left panel). When processed with external attitude measurements, the agreement between the LADCP and SADCPC velocity estimates improves greatly, with nearly 75% of the resulting per-station rms velocity differences below 0.06 m s^{-1} (right panel), indicating high quality.

5. Discussion and conclusions

The results presented above indicate that LADCP velocity profiles can be improved significantly by processing with 3D magnetometer and accelerometer measurements made with common microelectromechanical systems (MEMS) sensors. We have used an external self-contained datalogger to record these ancillary

measurements, but the same methodology can be applied to data collected with ADCPs that also record 3D magnetometer and accelerometer data. In the case of the ECOGIG profiles, the external attitude measurements reveal large compass errors in the uplooker ADCP as the main reason for the heading differences in the original ADCP data files. When processed with the external attitude measurements, the discrepancies between SADCPC and LADCP velocities reduce by 10%–20%. Based on observed compass differences from thousands of additional available dual-headed profiles, we expect similar improvements in other LADCP datasets.

While the improvements in the ECOGIG LADCP data quality is certainly welcome, it is important to note that the improvements are relatively modest, indicating that even without the external attitude data most profiles are of high quality. The main reason why compass errors do not contaminate regular LADCP profiles more fatally is that compass errors are heading dependent and average to zero; package rotation during the casts ensures that the same velocity is sampled at different instrument headings, thus averaging out the compass errors to some degree. Averaging the heading data from the two instruments further mitigates the problem for dual-headed LADCP systems. We conclude that for regular LADCP work external attitude measurements are optional.

The main benefit of using external attitude measurements is that they allow processing of LADCP profiles with bad attitudes. In the case of NABOS, the ADCP heading measurements are invalid because of a combination of a weak horizontal geomagnetic field and heavy sea state (there are many similar unprocessable profiles

from the Southern Ocean in the LDEO LADCP data archive). When processed with external attitude data, most of the resulting velocity profiles are of high quality. It is expected that even better profiles are possible with dual-headed LADCP systems.

We envision several further improvements to the instrument and methodology described here. Support for additional magnetometer and accelerometer chips can be easily added to the IMP firmware. For future deployments we plan to add gyroscopes to distinguish instrument tilt from horizontal acceleration, with the eventual goal of replacing the magnetometer with fiber-optic gyroscopes to remove the effects of magnetic disturbances, especially near the sea surface, and to allow collection of LADCP data arbitrarily close to the magnetic poles.

Acknowledgments. Part of this research was made possible by a grant from the Gulf of Mexico Research Initiative to support the Ecosystem Impacts of Oil and Gas Inputs to the Gulf (ECOGIG-2) research consortium. Funding for acquisition of the 2015 Arctic data was provided by NSF (1203473 and 1249133) and NOAA (NA15OAR4310155) under the NABOS-II program. Development of the prototype external magnetometer/accelerometer package (IMP) and methodology was carried out without external funding; extensive testing was carried out during cruises of the NSF-funded DIMES project (OCE-1232962). Participation of Ilona Goszczko on the NABOS cruise was made possible by the Polish National Science Center MIXAR project (2012/05/N/ST10/03643) and by funding from the Leading National Research Centre (KNOW) to the Centre for Polar Studies for the period 2014–18. Overall responsibility for CTD data acquisition and processing by Joe Montoya and Igor Polyakov for the Gulf of Mexico and Arctic CTD data, respectively, is gratefully acknowledged, as is the support by Piotr Wiczorek (IOPAN) for adapting an old ADCP pressure case and power supply for use with the IMP. The ECOGIG EN586 LADCP data are publicly available through the Gulf of Mexico Research Initiative Information and Data

Cooperative (GRIIDC; <https://data.gulfresearchinitiative.org>; doi:10.7266/N7K072BN). The 2015 NABOS LADCP data are available on request from the authors.

REFERENCES

- Firing, E., and R. Gordon, 1990: Deep ocean acoustic Doppler current profiling. *Proceedings of the IEEE Fourth Working Conference on Current Measurement*, IEEE, 192–201, doi:10.1109/CURM.1990.110905.
- Fischer, J., and M. Visbeck, 1993: Deep velocity profiling with self-contained ADCPs. *J. Atmos. Oceanic Technol.*, **10**, 764–773, doi:10.1175/1520-0426(1993)010<0764:DVPWSC>2.0.CO;2.
- Gregg, M. C., 1989: Scaling turbulent dissipation in the thermocline. *J. Geophys. Res.*, **94**, 9686–9698, doi:10.1029/JC094iC07p09686.
- Hamilton, J. M., 2001: Accurate ocean current direction measurements near the magnetic poles. The Proceedings of the Eleventh (2001) International Offshore and Polar Engineering Conference, J. S. Chung et al., Eds., Vol. 1, ISOPE, 656–660.
- Polzin, K. L., A. C. Naveira Garabato, T. N. Huussen, B. M. Sloyan, and S. Waterman, 2014: Finescale parameterizations of turbulent dissipation. *J. Geophys. Res. Oceans*, **119**, 1383–1419, doi:10.1002/2013JC008979.
- RD Instruments, 1998: ADCP coordinate transformation: Formulas and calculations. RDI Manual P/N 951-6079-00, 29 pp.
- St. Laurent, L., A. C. Naveira Garabato, J. R. Ledwell, A. M. Thurnherr, J. M. Toole, and A. J. Watson, 2012: Turbulence and diapycnal mixing in Drake Passage. *J. Phys. Oceanogr.*, **42**, 2143–2152, doi:10.1175/JPO-D-12-027.1.
- Thurnherr, A. M., 2010: A practical assessment of the errors associated with full-depth LADCP profiles obtained using Teledyne RDI Workhorse acoustic Doppler current profilers. *J. Atmos. Oceanic Technol.*, **27**, 1215–1227, doi:10.1175/2010JTECHO708.1.
- , 2011: Vertical velocity from LADCP data. *2011 IEEE/OES Tenth Current, Waves and Turbulence Measurements (CWTM)*, IEEE, 198–204, doi:10.1109/CWTM.2011.5759552.
- , J. R. Ledwell, J. W. Lavelle, and L. S. Mullineaux, 2011: Hydrography and circulation near the crest of the East Pacific Rise between 9° and 10°N. *Deep-Sea Res. I*, **58**, 365–376, doi:10.1016/j.dsr.2011.01.009.
- , L. St. Laurent, K. J. Richards, J. M. Toole, E. Kunze, and A. Ruiz Angulo, 2015: Vertical kinetic energy and turbulent dissipation in the ocean. *Geophys. Res. Lett.*, **42**, 7639–7647, doi:10.1002/2015GL065043.
- Visbeck, M., 2002: Deep velocity profiling using lowered acoustic Doppler current profilers: Bottom track and inverse solutions. *J. Atmos. Oceanic Technol.*, **19**, 794–807, doi:10.1175/1520-0426(2002)019<0794:DVPULA>2.0.CO;2.